

THE STOPPING POWER OF NEON IONS IN ALUMINUM

by

613-8302

KENDAHL CURTIS SHANE

B. S., McMaster University, 1969

---

A MASTER'S THESIS

submitted in partial fulfillment of the

requirements for the degree

MASTER OF SCIENCE

Department of Physics

KANSAS STATE UNIVERSITY

Manhattan, Kansas

1973

Approved by:

G. J. Lesman  
Major Professor

LD  
2668  
T4  
1973  
S525  
C.2  
Docu-  
ment

## TABLE OF CONTENTS

|                                    | PAGE |
|------------------------------------|------|
| LIST OF TABLES . . . . .           | iii  |
| LIST OF FIGURES . . . . .          | iv   |
| CHAPTER                            |      |
| I. INTRODUCTION . . . . .          | 1    |
| II. NEON ION ENERGY LOSS . . . . . | 4    |
| III. ELECTRONICS . . . . .         | 7    |
| IV. TARGET THICKNESS . . . . .     | 10   |
| V. ANALYSIS . . . . .              | 13   |
| VI. CHARGE EQUILIBRIUM . . . . .   | 22   |
| VII. CONCLUSION . . . . .          | 23   |
| REFERENCES . . . . .               | 25   |
| ACKNOWLEDGMENTS . . . . .          | 26   |
| ABSTRACT                           |      |

## LIST OF TABLES

| TABLE  | PAGE |
|--|------|
| 1. Target thicknesses . . . . .                  | 12   |
| 2. Results of energy loss measurements . . . . . | 20   |
| 3. Summary of stopping power results . . . . .   | 21   |

## LIST OF FIGURES

| FIGURE   | PAGE |
|--|------|
| 1. Energy levels and decay scheme of $^{20}\text{Ne}$ . . . . .    | 3    |
| 2. Schematic of target chamber and detectors . . . . .             | 5    |
| 3. Schematic of the electronics . . . . .                          | 8    |
| 4. Doppler-shifted gamma peaks obtained in measurement 1 . . . . . | 14   |
| 5. Doppler-shifted gamma peaks obtained in measurement 2 . . . . . | 15   |
| 6. Doppler-shifted gamma peaks obtained in measurement 3 . . . . . | 16   |
| 7. Doppler-shifted gamma peaks obtained in measurement 4 . . . . . | 17   |
| 8. Stopping power of Ne ions in aluminum . . . . .                 | 24   |

## CHAPTER I

### INTRODUCTION

Stopping powers have been studied extensively for many years, but the complexity of the phenomena involved is such that there remain serious discrepancies between theory and experiment and among various experiments. For the case of Ne ions in aluminum, Northcliffe's measurements<sup>1</sup> fall significantly below the standard curve of Northcliffe and Schilling<sup>2</sup> based on a compilation of available data. Thus, there is still a need for new and independent experimental data.

When a heavy ion passes through a medium, it loses kinetic energy through collisions with the atoms and electrons in the medium. In the case of an ion passing through a thin foil, the energy loss,  $\Delta E$ , is given by

$$\Delta E = \frac{m}{2} (v_i^2 - v_f^2) \quad (1)$$

where  $m$  is the mass of the ion, and  $v_i$  and  $v_f$  are, respectively, the ion's initial and final velocities. That is,  $v_i$  is its velocity before it enters the foil, and  $v_f$  is its velocity after it leaves the foil. If the moving ion's nucleus should gamma decay, the gamma energy observed is

$$\frac{\epsilon}{\epsilon_0} = \frac{\sqrt{1 - v^2/c^2}}{1 - \frac{v}{c} \cos \theta} \quad (2)$$

where  $\epsilon$  is the doppler-shifted gamma energy,  $\epsilon_0$  is the gamma energy in the nucleus' rest frame, and  $\theta$  is the angle between the direction of motion of the ion and the direction of propagation of the gamma ray. With a knowledge of  $\epsilon$ ,  $\epsilon_0$  and  $\theta$ , the ion's velocity may be calculated.

In this experiment, the energy lost by 20 MeV  $^{20}\text{Ne}$  ions in an aluminum

foil  $\sim 0.3 \text{ mg/cm}^2$  thick was measured by observing the doppler shifts in gamma rays from the 1.633 MeV first excited state of  $^{20}\text{Ne}$ . From this information the stopping power was calculated. As will be shown, the results are in agreement with the best semi-empirical estimates of Ne stopping powers presently available.

**THIS BOOK  
CONTAINS  
NUMEROUS PAGES  
WITH DIAGRAMS  
THAT ARE CROOKED  
COMPARED TO THE  
REST OF THE  
INFORMATION ON  
THE PAGE.**

**THIS IS AS  
RECEIVED FROM  
CUSTOMER.**

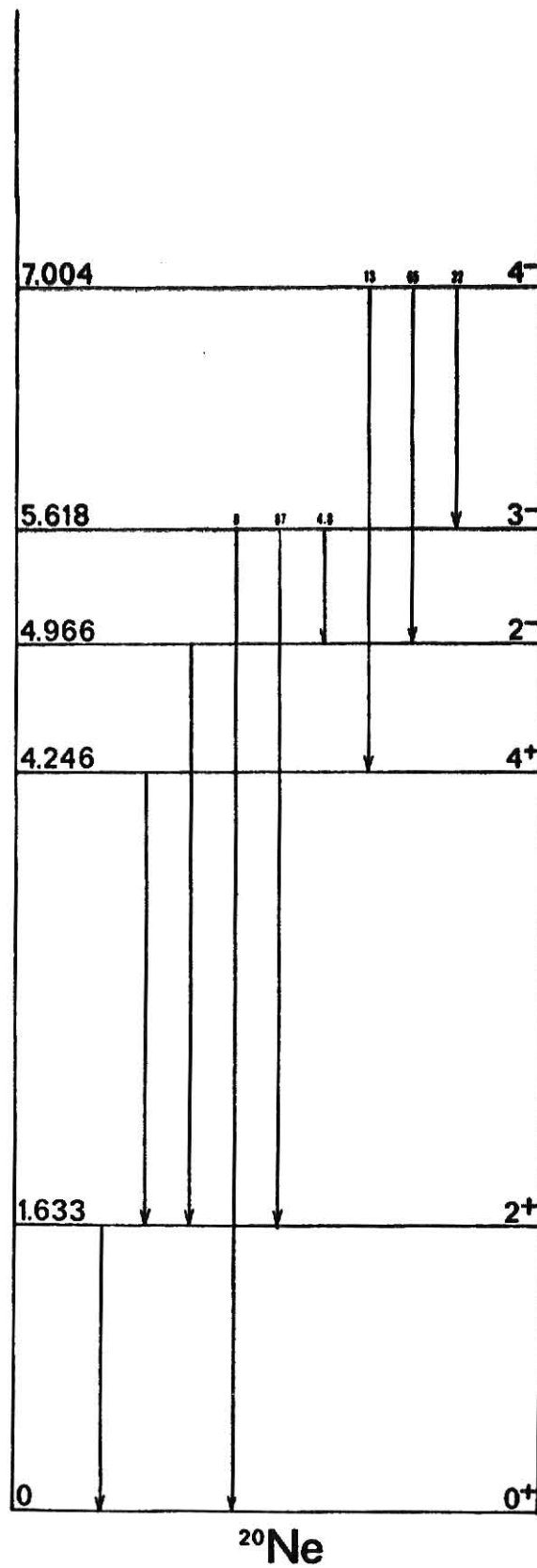


Fig. 1: Energy levels and decay scheme of  $^{20}\text{Ne}$



## CHAPTER II

### NEON ION ENERGY LOSS

$^{20}\text{Ne}$  ions were produced in the chamber pictured in Fig. 2 by the reaction  $^{12}\text{C}(^{12}\text{C},\alpha)^{20}\text{Ne}$ , using the  $^{12}\text{C}$  beam from the K.S.U. model EN tandem Van de Graff accelerator. Alpha particles were detected with an annular silicon surface barrier detector subtending angles of  $165^\circ$  to  $176^\circ$ , and gamma rays were detected with a Ge(Li) detector. Fast-slow coincidence logic (Fig. 3) was used to obtain spectra of gamma rays in coincidence with alpha particles from the decay of the compound system to the first excited state of  $^{20}\text{Ne}$ . These spectra were accumulated in a Canberra model 8050 analog-to-digital converter interfaced to a 4096-channel TMC analyzer, transferred to the memory of a PDP-15 computer, and stored on magnetic tape. Since the coincidence alpha particles were observed at angles greater than  $165^\circ$ , the coincidence gammas came from Ne ions moving at less than  $3^\circ$ ; that is, their motion was essentially normal to the target. The energy of the recoil  $^{20}\text{Ne}$  ions was 20 MeV with a  $^{12}\text{C}$  projectile energy of 21.2 MeV.

Gamma coincidence spectra were taken from two different kinds of targets in each energy loss measurement. One was a self-supporting, natural carbon foil  $\sim 20 \mu\text{g}/\text{cm}^2$  thick. The velocity of the Ne ions contributing to the coincidence spectrum was taken to be  $v_i$ . The other kind of target was  $\sim 25 \mu\text{g}/\text{cm}^2$  of natural carbon backed by an aluminum foil  $\sim 0.3 \text{ mg}/\text{cm}^2$  thick. The time for 20 MeV Ne ions to go through the foil is 0.08 ps, while the lifetime of the first excited state of  $^{20}\text{Ne}$  is 1.2 ps so that 94% of the coincidence gammas came from ions which had left the foil before decaying,

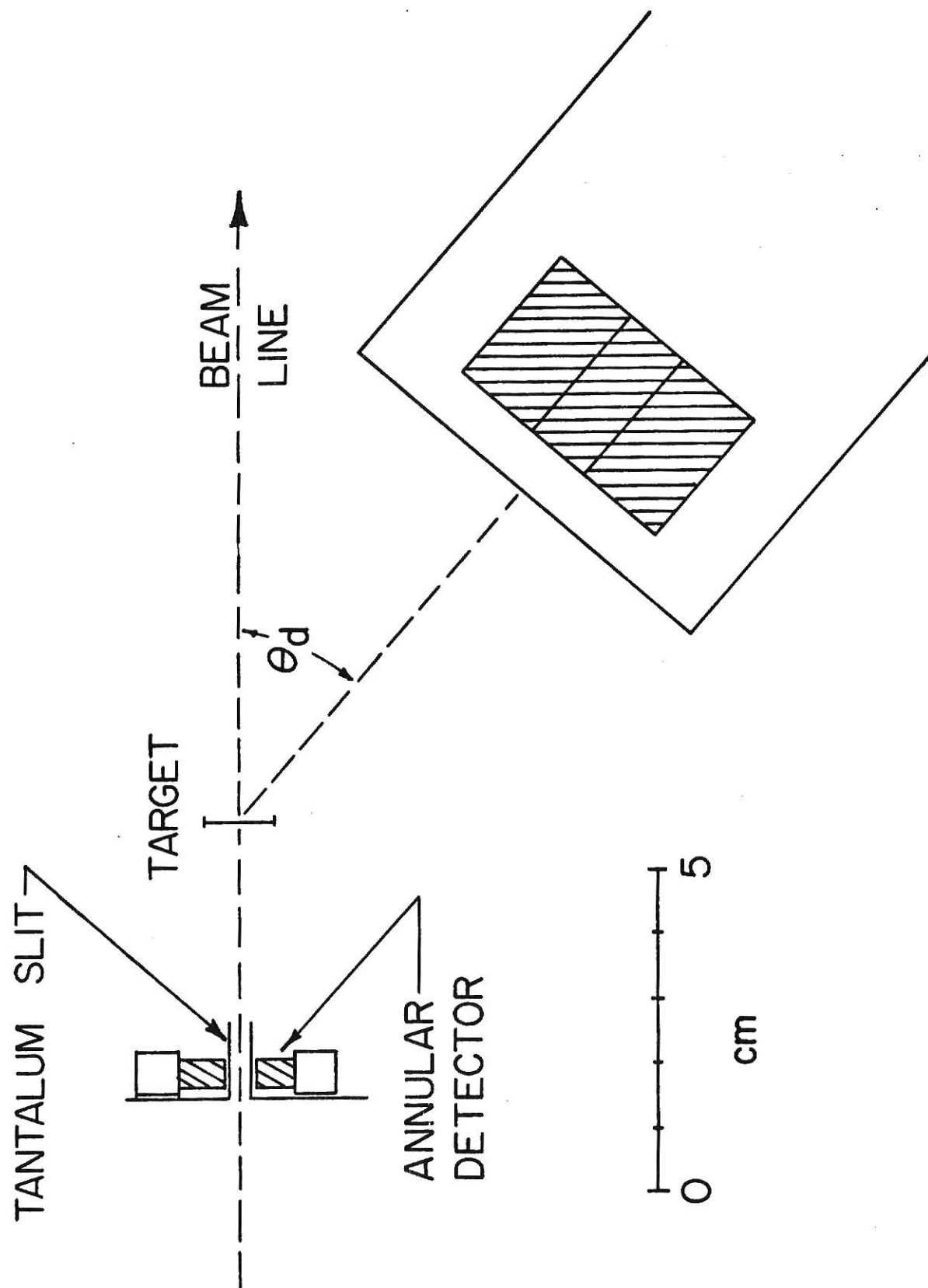


Fig. 2: Schematic of target chamber and detectors

and which, therefore, were travelling at their final velocity,  $v_f$ . The effect on the spectrum of the 6% which decayed while still in the foil was estimated by calculating a histogram of the peak. These decays provide a high energy tail to the sharp main peak due to the other 94%. This tail was found to be small compared to the main peak and completely indistinguishable from the random coincidence background. It was, therefore, not included in determining the centers of the doppler-shifted gamma peaks.

If the thickness of the self-supporting carbon foil was much different from that of the carbon layer on the aluminum-backed target, the measured  $v_i$  would not represent the velocity of the Ne ions as they entered the aluminum, thereby introducing a systematic error into the energy loss result. To check on this possibility, the carbon thicknesses were measured as described in Chapter IV. The results, which are given in Table 1, imply a maximum systematic error of  $0.05 \pm .02$  MeV, which is completely negligible.

Four energy-loss measurements were made on two aluminum-backed targets. Two of these were made on one target (henceforth called number I) and used alpha particles scattered to the first excited state. The third measurement, made on another target (number II), also used first-excited-state alphas. The fourth and final measurement, made on target II, used alphas to the 4.246 MeV second excited state of  $^{20}\text{Ne}$ . Using second-state alphas, instead of first-state alphas, reduced the Ne ions' kinetic energy by 1.3 MeV, and very slightly increased the time from formation of the second state to gamma decay of the first state, since the  $4^+$  second state, with a lifetime of  $0.093 \text{ ps}^3$ , de-excites by way of the  $2^+$  first state.

## CHAPTER III

### ELECTRONICS

Standard "fast-slow" coincidence logic (Fig. 3) was used in taking data. Signals from the preamplifier on the gamma detector were amplified by a Tennelec TC-200 amplifier and sent to a Canberra model 8050 analog-to-digital converter (ADC), which performed a pulse height analysis on them. Gain stabilization was used only with measurements 3 and 4.

To select the alpha particle associated with a particular gamma ray, signals from the Tennelec preamplifier (alphas) and the fast output of the TC-200 amplifier (gammas) were amplified and sent through fast discriminators to provide start and stop pulses for a time-to-amplitude converter (TAC). The output of the TAC is a pulse whose height is proportional to the elapsed time between the start and stop pulses. This is the "fast" part of the system. The TAC output went to two single channel analyzers (SCA). The window of one SCA was set on the coincidence peak to determine true coincidences. The window of the other SCA was set away from the peak to determine the number of accidental coincidences lying under the true coincidence peak.

Part of the alpha preamplifier signal was amplified and sent to a timing single channel analyzer (TSCA) to pick out alpha decays to the first (or second) excited state of  $^{20}\text{Ne}$ . Its output went to two overlap coincidence units (OC). The second coincidence input to one of the OC's came from the "accidentals" SCA. An output pulse from this OC, which was counted by a scaler, indicated an accidental coincidence with a first (or second) state alpha particle. The second coincidence input to the other OC came from the

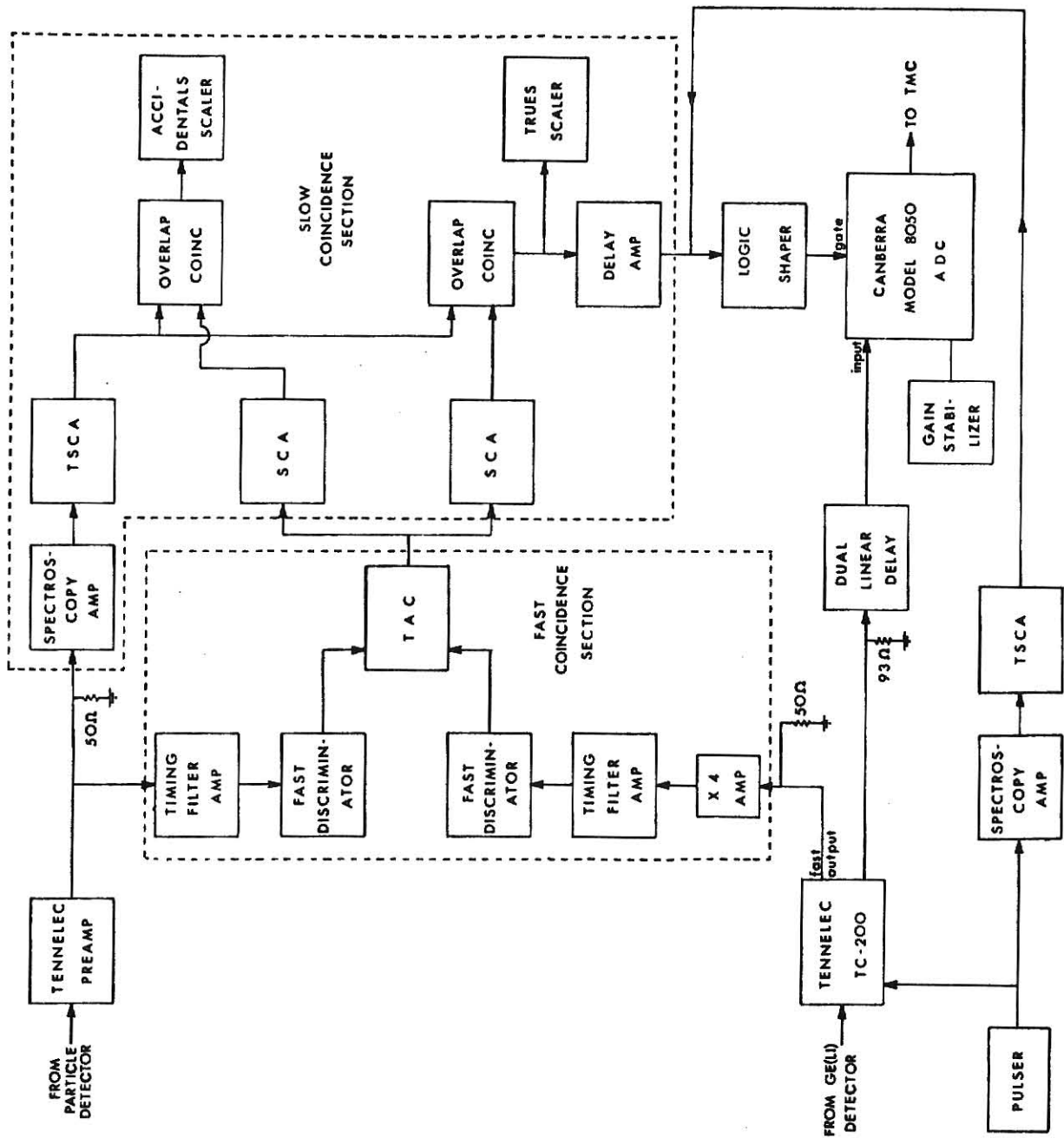


Fig. 3: Schematic of the electronics

"trues" SCA. This OC's output was used to gate the ADC and to drive a scaler which counted the true coincidences.

In the limit of low alpha and gamma count rates ( $\sim 1000/\text{sec}$ ), events are well separated on the time scale of slow coincidence electronics and fast coincidence is not needed. However, much higher count rates are required for a coincidence experiment to be feasible. Slow coincidence times are a few microseconds, while the resolving time of the fast coincidence used here was about 50 nanoseconds. Because of this improved temporal resolution the background in the gamma coincidence spectrum due to accidental coincidences was lowered by a factor of one hundred.

The gain stabilization system consisted of a precision pulser fed into an input of the TC-200 and a gain stabilizer connected to the ADC and set to monitor the pulser's location in the coincidence gamma spectrum. The pulser signal was also sent to an SCA which gated the ADC so that the pulser's signals from the TC-200 would be accepted by the ADC and analyzed. If the gain of the system happened to drift, the stabilizer sensed the change in the location of the pulser peak and supplied an appropriate analog correction to the ADC, which was added to the input signal before analysis. When working properly, the gain stabilization system reduced troublesome temperature-dependent gain shifts to less than 0.2 channels.

## CHAPTER IV

### TARGET THICKNESS

A thick carbon reference foil was made by mounting two carbon foils, each purported to be  $40 \mu\text{g}/\text{cm}^2$  thick, one on top of the other. The thickness of this foil was determined by measuring the energy lost in it by 5.486 MeV alpha particles from a collimated  $^{241}\text{Am}$  source. The stopping power of these alphas in carbon is given by the stopping power tables in the Nuclear Data Tables<sup>2</sup> as  $0.770 \text{ MeV}/(\text{mg}/\text{cm}^2) \pm 5\%$ . From this value and the measured energy loss, the reference foil was found to be  $108 \pm 8 \text{ mg}/\text{cm}^2$  thick.

Protons with an energy of 2 MeV were elastically scattered from the reference foil, from the self-supporting carbon foil and from targets I and II. The scattered protons were observed at an angle of  $150^\circ$  so that the peaks due to scattering from carbon, oxygen and aluminum would be resolved. The thickness of carbon is proportional to the scattering yield, with the known thickness of the reference foil providing a calibration point. Since the scattering measurements were performed with the same projectile energy and scattering angle and only the targets were changed, the relationship between the thickness and scattering yield does not require any assumptions about the scattering cross section. The results for the thicknesses of the carbon components of targets I and II and of the self-supporting foil are given in Table 2.

A measurement was made of the energy lost in targets I and II by alpha particles from the  $^{241}\text{Am}$  source. With a knowledge of the thickness of the carbon component of each target, the energy lost in the carbon component

could be determined and subtracted from the total energy loss to give the energy lost in the aluminum component. From the Nuclear Data Tables<sup>2</sup>, the stopping power of 5.486 MeV alpha particles in aluminum is  $0.566 \text{ MeV}/(\text{mg}/\text{cm}^2) \pm 5\%$ . The thicknesses of the aluminum components follow directly and are given in Table 2.



| Target                      | Alpha<br>energy loss<br>(MeV) | Thickness of<br>carbon<br>( $\mu\text{g}/\text{cm}^2$ ) | Thickness of<br>aluminum<br>( $\text{mg}/\text{cm}^2$ ) |
|-----------------------------|-------------------------------|---|---|
| I                           | $0.197 \pm .006$              | $28 \pm 2$  | $0.31 \pm .02$  |
| II                          | $0.182 \pm .006$              | $25 \pm 2$  | $0.29 \pm .02$  |
| self-supporting carbon foil |                               | $20 \pm 3$  |   |

Table 1: Target thicknesses

## CHAPTER V

### ANALYSIS

The coincidence spectra obtained in the energy loss measurements are presented in Fig. 4 - 7. Each pair of carbon target and aluminum-backed target spectra from the same measurement is plotted with the same energy axis so that the relative shift of the peaks is apparent.

The centers of these peaks were taken to be their centroids, defined as

$$C = \frac{\sum n(Y_n - B_n)}{\sum (Y_n - B_n)} \quad (3)$$

where  $C$  is the centroid,  $Y_n$  is the number of counts in channel  $n$ , and  $B_n$  is the number of background counts in that channel. The sums are taken across the peak. The centroid error,  $\delta C$ , is given by

$$(\delta C)^2 = \frac{\sum (n-C)^2 [(\delta Y_n)^2 + (\delta B_n)^2]}{\sum (Y_n - B_n)} \quad (4)$$

where  $\delta Y_n = \sqrt{Y_n}$  and  $\delta B_n$  = standard deviation of the least squares fit to the background.

Unless a peak is symmetric, its center and its centroid do not coincide. For gamma ray spectra obtained in this experiment, the energy uncertainty arising from this difference was negligible compared to the error in the gamma ray energy. However, when the shift between two peaks very close to each other is considered, even this small error is liable to be significant. If the shapes of the two peaks are the same, the errors cancel, and the value obtained for the shift is correct. A chi square test on the coincidence peaks from the first measurement showed that their shapes were indeed the same.

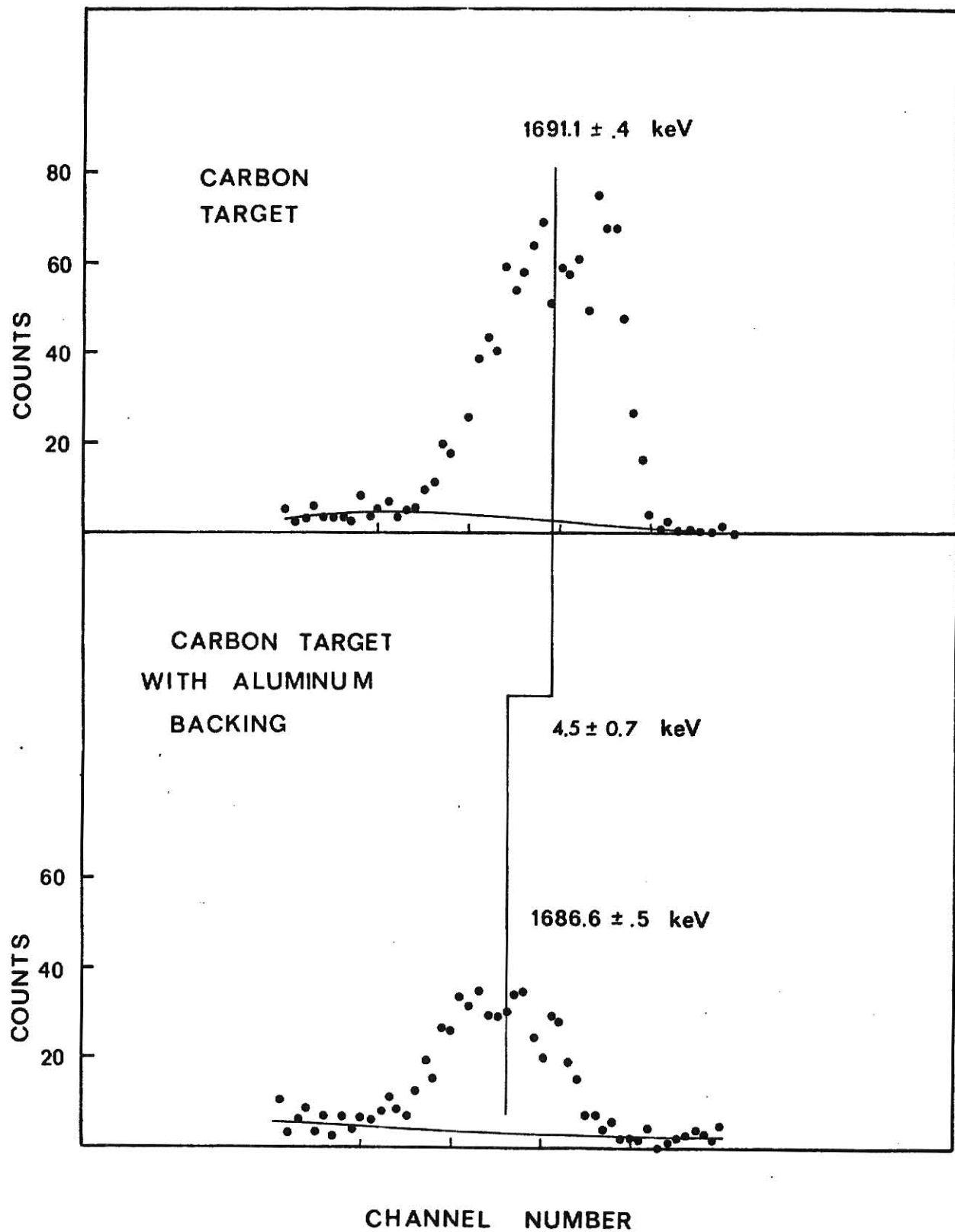


Fig. 4: Doppler-shifted gamma peaks obtained in measurement 1

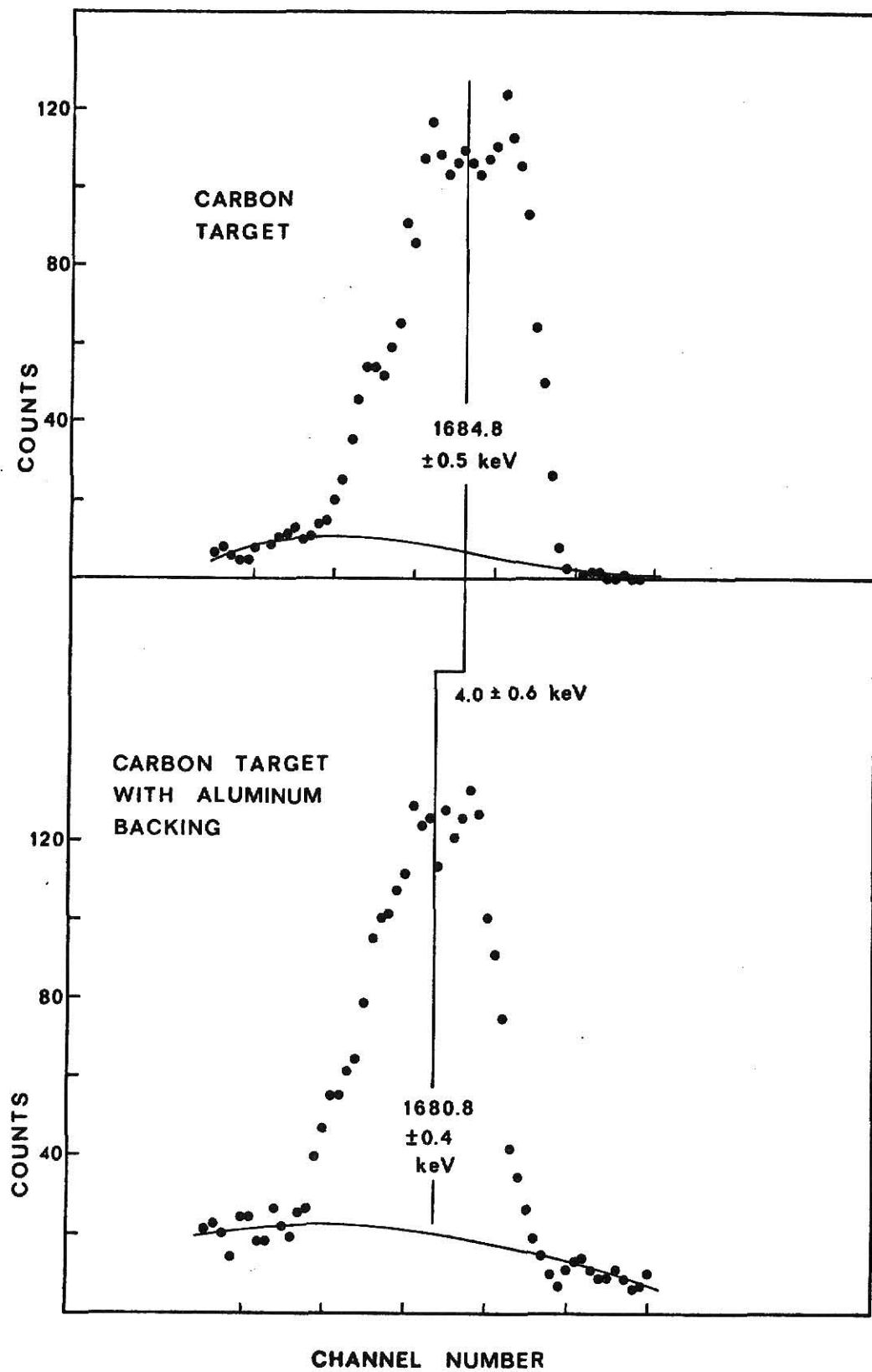


Fig. 5: Doppler-shifted gamma peaks obtained in measurement 2

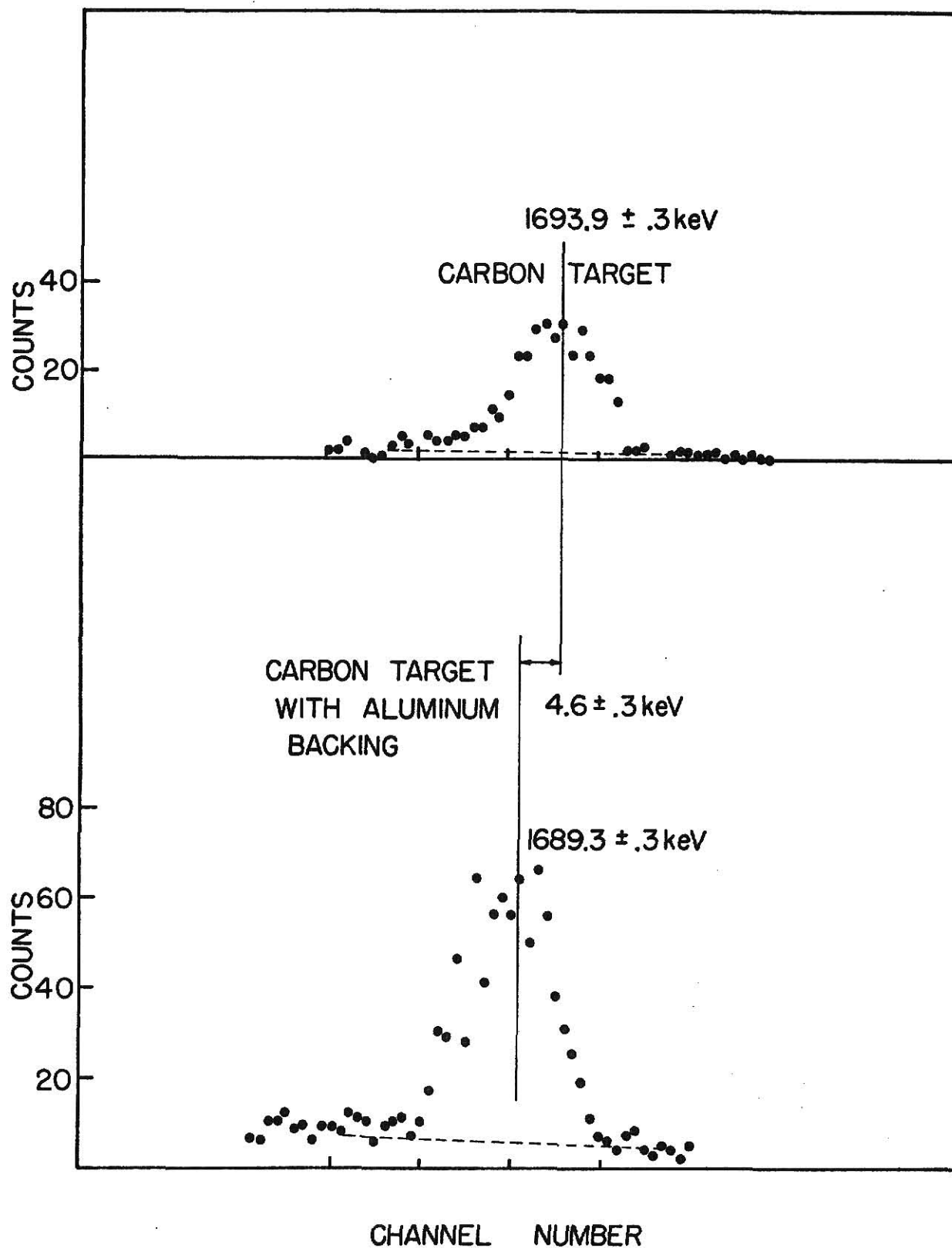


Fig. 6: Doppler-shifted gamma peaks obtained in measurement 3

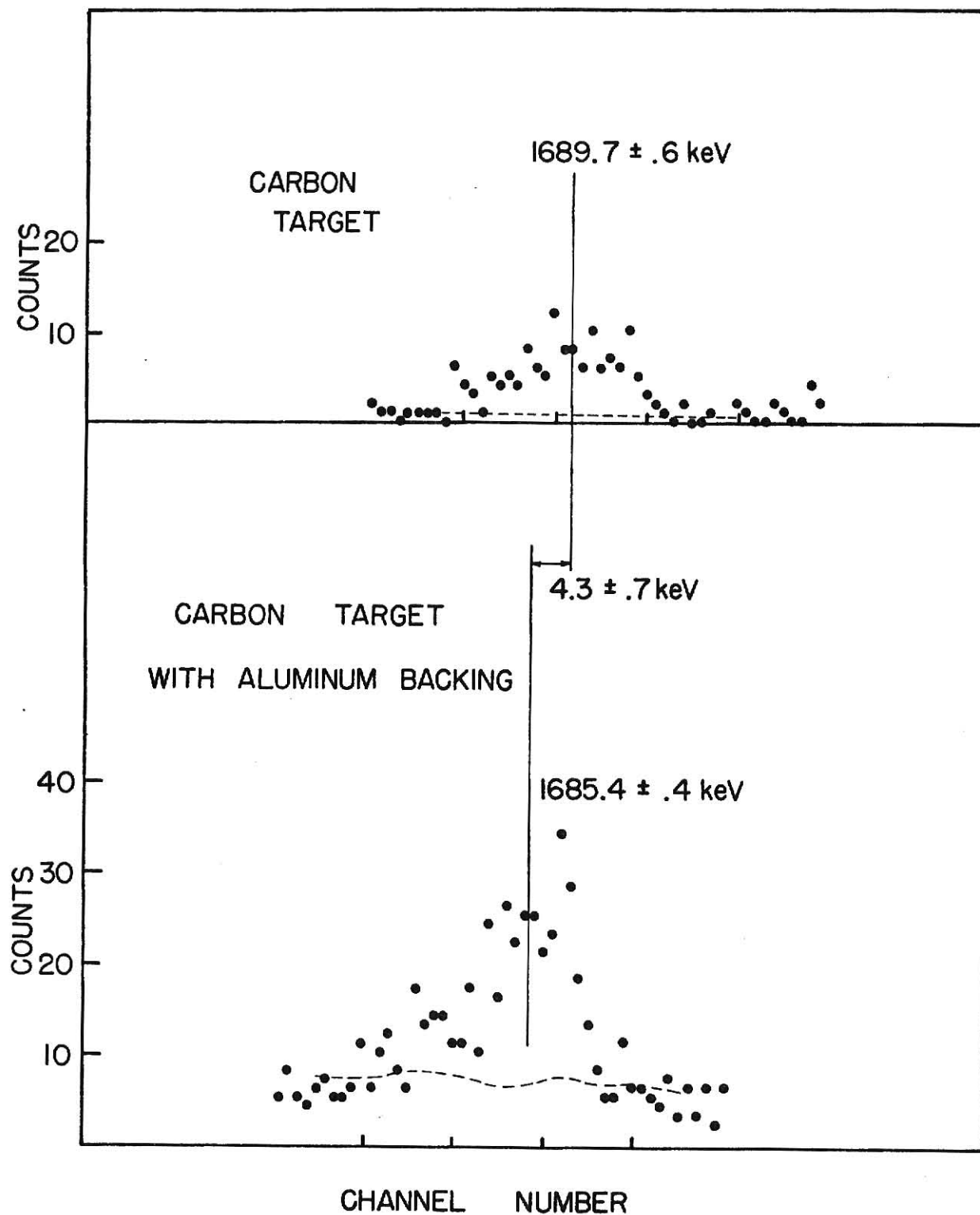


Fig. 7: Doppler-shifted gamma peaks obtained in measurement 4

Backgrounds were fitted to all peaks using the least squares method. For the first two measurements, cubic backgrounds were fitted to a few channels on either side of the coincidence peaks. For the third and fourth measurements, direct gamma ray spectra (singles spectra) were taken from both carbon and aluminum-backed targets, and were scaled to fit a few channels on the high energy side of the coincidence peaks. Since the accidental coincidence spectrum should be the same shape as a singles spectrum, this method represents a way of correcting for accidentals, but with better statistics than that of the actual accidentals spectrum.

Singles spectra from  $^{60}\text{Co}$  and  $^{88}\text{Y}$  sources were used for calibration. The calibration points were the 1332.48 keV gamma from  $^{60}\text{Ni}$  and the 1836.2 keV gamma from  $^{88}\text{Sr}$ . Their centroids, calculated with cubic backgrounds, were taken to be their centers. In view of the gain shifts during the coincidence runs, the errors assigned to some of the calibrations are larger than those given by equation (4). During the second measurement, gain shifts were large enough so that it was necessary to collect coincidence data for ~10 hours, store it, take a calibration spectrum and start a fresh coincidence spectrum. The coincidence spectra for this measurement, shown in Fig. 5, are the combined results, with all the contributions corrected to the same gain before being added in. Gain shifts in the first measurement were non-negligible, but not so large as to require this piece-meal approach. During the third and fourth measurements, a Canberra gain stabilizer was used in conjunction with a precision pulser to eliminate the gain shift problem.

With the following definitions:

$$\epsilon_y = {}^{88}\text{Y energy} = 1836.2 \pm .1 \text{ keV,}$$

$N_y$  =  $^{88}\text{Y}$  channel number,

$\epsilon_c$  =  $^{60}\text{Co}$  energy =  $1332.48 \pm .01$  keV,

$N_c$  =  $^{60}\text{Co}$  channel number,

$\epsilon_d$  = energy of doppler-shifted gamma,

$N_d$  = channel number of doppler-shifted gamma,

the energy of a doppler-shifted gamma ray is

$$\epsilon_d = \epsilon_c + \frac{\epsilon_y - \epsilon_c}{N_d - N_c} (N_d - N_c) \quad (5)$$

The gamma energy results are given in Table 2. On using them in equation (2) and solving numerically, one obtains  $v_i$  and  $v_f$  for each measurement. Values for the energy loss then follow from equation (1). These results are also given in Table 2.

With a knowledge of the energy lost in the aluminum foil by the Ne ions and the foil thickness, a value for the stopping power follows by simple division. The stopping power results are summarized in Table 3.



| Measurement<br>number | Doppler-shifted $\gamma$ ray energies (keV)<br>C target | Al-backed target | Ge(Li) angle<br>(degrees) | Ne ion energy<br>loss (MeV) |
|-----------------------|---|------------------|---------------------------|-----------------------------|
| 1                     | 1691.1 $\pm$ .4   | 1686.6 $\pm$ .5  | 41 $\pm$ 1                | 3.0 $\pm$ .5                |
| 2                     | 1684.8 $\pm$ .5   | 1680.8 $\pm$ .4  | 48.0 $\pm$ .5             | 3.1 $\pm$ .5                |
| 3                     | 1693.4 $\pm$ .3   | 1689.4 $\pm$ .2  | 38.5 $\pm$ 2              | 2.6 $\pm$ .3                |
| 4                     | 1689.8 $\pm$ .6   | 1684.7 $\pm$ .4  | 38.5 $\pm$ 2              | 3.1 $\pm$ .5                |

Table 2: Results of energy loss measurements

| Measurement<br>number | Ne ion energy<br>(MeV) | $\Delta E/\Delta x$<br>(MeV/(mg/cm <sup>2</sup> )) |                             |
|-----------------------|------------------------|--|-----------------------------|
| 1                     | 18                     | $9.6 \pm 1.6$                                      | target I, 1st state alphas  |
| 2                     | 18                     | $9.9 \pm 1.7$                                      | target I, 1st state alphas  |
| 3                     | 18                     | $9.0 \pm 1.1$                                      | target II, 1st state alphas |
| 4                     | 17                     | $10.6 \pm 1.8$                                     | target II, 2nd state alphas |

Weighted mean stopping power of  
first three measurements =  $9.4 \pm .6$  MeV/(mg/cm<sup>2</sup>))

Table 3: Summary of stopping power results

## CHAPTER VI

### CHARGE EQUILIBRIUM

The Ne stopping powers measured in this experiment were compared with those given by Northcliffe and Schilling<sup>2</sup> for protons of the same velocity (the same  $E/A$ ) in aluminum. From this, the equilibrium charge on the Ne ions was found to be  $+7.1 \pm .3$  for 18 MeV ions and  $+7.4 \pm .7$  for 17 MeV ions. These results compare well with the calculated values of +7.5 and +7.3, respectively, given by Marion<sup>4</sup>, and with the value  $+7.6 \pm .8$ , measured by Northcliffe<sup>1</sup>.

Since stopping power is proportional to  $Z^2$ , the square of the charge on the projectile, it is important that the equilibrium value of  $Z^2$  be achieved quickly. While the charge exchange process leading to equilibrium has been studied extensively in gases, there is little data available for solids. Teplova et al.<sup>5</sup> report that 8.8 MeV N ions reach equilibrium in 3 - 4  $\mu\text{g}/\text{cm}^2$  of celluloid. Moak et al.<sup>6</sup> have studied the approach to equilibrium of 140 MeV  $\text{Br}^{(15+)}$  ions in carbon. Their results indicate that  $Z^2$  for these ions comes within 10% of its equilibrium value after 8  $\mu\text{g}/\text{cm}^2$ . Since the aluminum foils used in this experiment are 300  $\mu\text{g}/\text{cm}^2$  thick, the energy loss measured is insensitive to the details of the Ne ions' approach to charge equilibrium.

## CHAPTER VII

### CONCLUSION

The results of this experiment are compared in Fig. 8 with the standard stopping power curve<sup>2</sup>, and with Northcliffe's measurements<sup>1</sup>. For Ne ions in aluminum, the standard curve is a semi-empirical fit to experimental results guided by theoretical relationships. Near 20 MeV, the fit was made to Northcliffe's data, which was obtained by measuring the energy lost by a Ne beam in aluminum foils of known thickness.

The results of the present experiment are clearly in agreement with the standard curve while contradicting the trend of Northcliffe's results, which suggest lower values for the stopping power.

Previously, if the stopping power of an ion was to be measured, it was necessary to produce a beam of ions with the desired energy. The advantage of this new technique is that a beam of Ne ions did not have to be accelerated. Thus, using various reactions, the number of ions for which direct stopping power measurements can be made may be considerably increased.

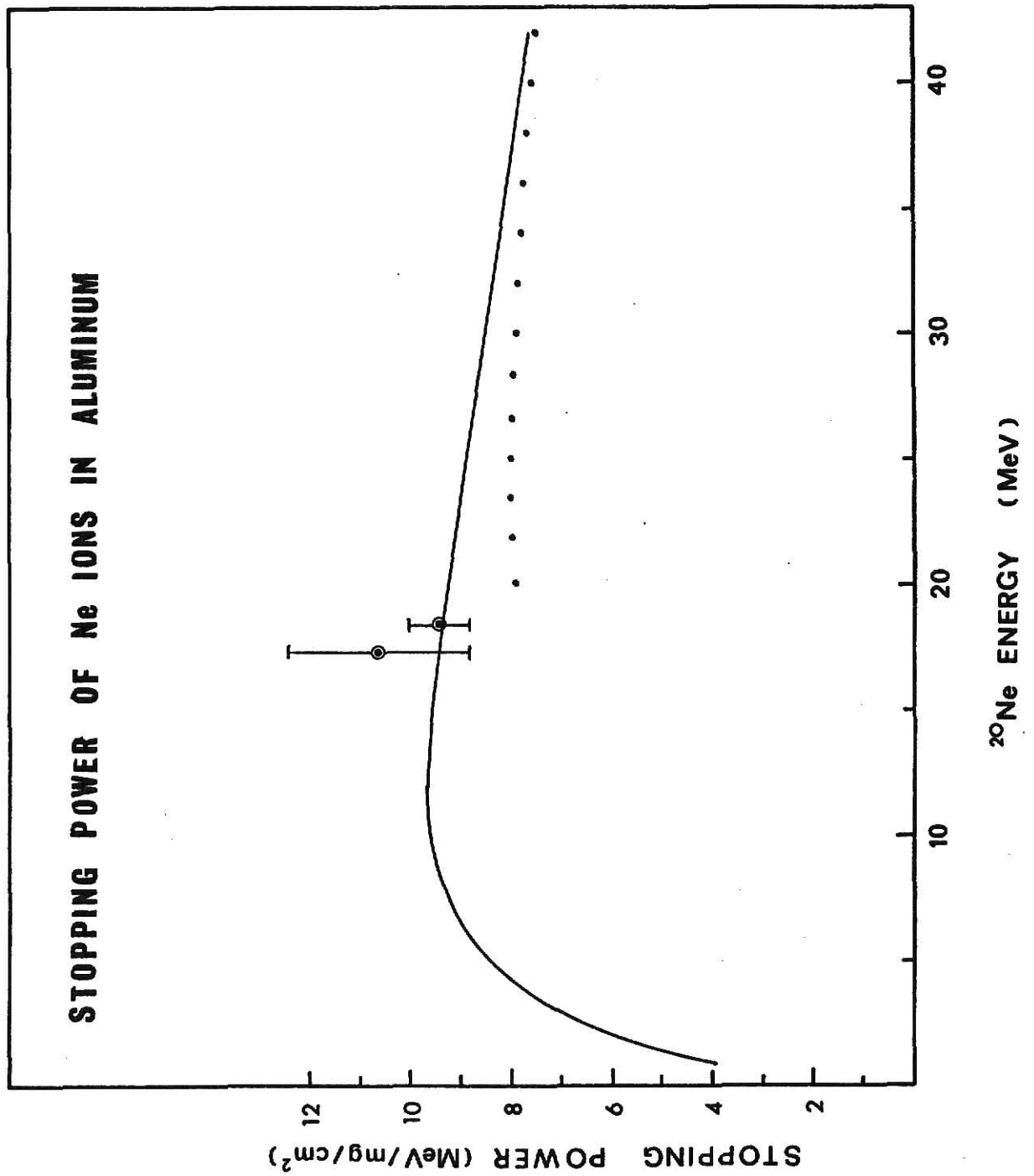


Fig. 8: Stopping power of Ne ions in aluminum

## REFERENCES

- 1) L. C. Northcliffe, Phys. Rev. 120, 1744 (1960).
- 2) L. C. Northcliffe and R. F. Schilling, Nuclear Data Tables A7, 233 (1970).
- 3) O. Häusser, T. K. Alexander, A. B. McDonald, G. T. Ewan and A. E. Litherland, Nuclear Physics A168, 17 (1971).
- 4) J. B. Marion and F. C. Young, Nuclear Reaction Analysis, (North Holland, Amsterdam, 1968), p. 45.
- 5) Ya. A. Teplova, I. S. Dmitriev and V. S. Nikolaev, Journal of Physics B4, L70 (1971).
- 6) C. D. Moak, H. O. Lutz, L. B. Bridwell, L. C. Northcliffe and S. Datz, Phys. Rev. Lett. 18, 41 (1967).

## ACKNOWLEDGMENTS

The author wishes to acknowledge the invaluable advice and assistance of Dr. Gregory Seaman, who originated this application of doppler shift measurements and who suggested this project. The efforts of Dr. John Brand, who made the aluminum-backed targets, and of Mr. Ron Keller, Dr. Helmut Laumer and Mr. Monty Volckmann, who helped during data taking, are also gratefully acknowledged.

THE STOPPING POWER OF NEON IONS IN ALUMINUM

by

KENDAHL CURTIS SHANE

B. S., McMaster University, 1969

---

AN ABSTRACT OF A MASTER'S THESIS

submitted in partial fulfillment of the

requirements for the degree

MASTER OF SCIENCE

Department of Physics

KANSAS STATE UNIVERSITY

Manhattan, Kansas

1973



## ABSTRACT

The stopping powers of 17 and 18 MeV Ne ions in aluminum have been measured by a new technique. The doppler shifts in  $^{20}\text{Ne}$  gamma rays were measured to find the initial and final velocities of Ne ions passing through thin aluminum foils of known thickness. The stopping powers were found to be  $10.6 \pm 1.8 \text{ MeV}/(\text{mg}/\text{cm})$  at 17 MeV and  $9.4 \pm .6 \text{ MeV}/(\text{mg}/\text{cm})$  at 18 MeV. These results are in agreement with the best semi-empirical estimates of Ne stopping powers that are presently available.